

# The Microbead Occlusion Model: A Paradigm for Induced Ocular Hypertension in Rats and Mice

Rebecca M. Sappington, Brian J. Carlson, Samuel D. Crish, and David J. Calkins

**PURPOSE.** Elevated intraocular pressure (IOP) is an important risk factor for glaucoma. Animal models often involve techniques for IOP elevation that are surgically invasive. Here the authors describe a novel and relatively simple method for inducing a highly consistent, modest, and repeatable elevation in IOP for rats and mice.

**METHODS.** IOP was elevated unilaterally by injection of polystyrene microbeads into the anterior chamber to occlude aqueous outflow in rats (2.5–7  $\mu$ L) and mice (1  $\mu$ L). The fellow eye received an equivalent saline injection as internal control. The authors used tonometry to measure microbead-induced IOP elevations. Optic nerves were processed histologically to determine axon loss.

**RESULTS.** For rats, a single injection of microbeads raised IOP by 21% to 34%, depending on volume, for approximately 2 weeks, though they were not tracked to full recovery. IOP in the saline-injected eye was constant. An additional injection (5  $\mu$ L) extended the elevation to 8 weeks. Cumulative pressure exposure for both injections increased linearly. For mice, a single 1- $\mu$ L injection of microbeads elicited a highly regular 30% elevation in IOP that persisted for more than 3 weeks, with a linear rise in cumulative pressure exposure. For both rats and mice, interanimal variability on a given day was modest, approximately 5% of the mean IOP measurement. Extended elevations (4–5 weeks) induced approximately a 20% loss of axons in both rats and mice.

**CONCLUSIONS.** These data support a novel and flexible model of modest ocular hypertension with axon loss. The maximal duration of IOP elevation will be further characterized in future studies. (*Invest Ophthalmol Vis Sci.* 2010;51:207–216) DOI: 10.1167/iovs.09-3947

From the Vanderbilt Eye Institute, Vanderbilt University Medical Center, Nashville, Tennessee.

Supported by the Melza M. and Frank Theodore Barr Foundation through the Glaucoma Research Foundation Catalyst for a Cure initiative (DJC); National Institutes of Health Grant EY017427 (DJC); a Departmental Unrestricted Grant and a Wasserman Award from Research to Prevent Blindness, Inc. (DJC); an American Health Assistance Foundation National Glaucoma Award (DJC); the Vanderbilt Discovery Science program (DJC); Vanderbilt Vision Research Center National Eye Institute Core Grant (5P30EY008126–19); and fellowships from Fight for Sight, Inc. (RMS, SDC).

Submitted for publication May 4, 2009; revised June 30, August 13, and September 22, 2009; accepted September 27, 2009.

Disclosure: **R.M. Sappington**, None; **B.J. Carlson**, None; **S.D. Crish**, None; **D.J. Calkins**, None

Corresponding author: David J. Calkins, Department of Ophthalmology and Visual Sciences, The Vanderbilt Eye Institute, Vanderbilt University Medical Center, Ophthalmology Research Lab, 1105 Medical Research Building IV, Nashville, TN 37232-0654; david.j.calkins@vanderbilt.edu.

Glaucoma is a common optic neuropathy characterized by the degeneration of retinal ganglion cells and their axons, which comprise the optic nerve. Although age is the most significant risk factor for the disease,<sup>1</sup> elevated intraocular pressure (IOP) remains the only modifiable risk factor.<sup>2</sup> In humans, whether open or closed angle, glaucoma is characterized by excavation of the optic disc and defects in the nerve fiber layer that are often accompanied by elevations in IOP.<sup>3</sup> Lowering IOP slows glaucomatous progression, even in patients with IOP in the nominally normal range (15–21 mm Hg).<sup>2</sup> Given the impact of IOP on disease outcome, elevated IOP or ocular hypertension is the predominant feature of most animal models of glaucoma.

Rodent species offer convenience as model systems for inducing ocular hypertension because they provide the opportunity to conduct large-scale experimental studies and the potential for genetic manipulations. The three most commonly used models elevate IOP substantially (50%–100% above baseline) by altering aqueous fluid dynamics in the anterior segment.<sup>4,5</sup> These have been applied primarily to rats, most likely because of the technical difficulty of manipulating the significantly smaller mouse eye.<sup>4–6</sup> Their merits and weaknesses have been reviewed extensively elsewhere.<sup>5</sup> Briefly, episcleral vein injection of hypertonic saline elevates IOP by altering aqueous outflow through sclerosis.<sup>7,8</sup> This elevation persists as long as 200 days but varies dramatically in magnitude between individual animals.<sup>5,7,9</sup> Laser photocoagulation of either the trabecular meshwork alone or in concert with episcleral veins elevates IOP for far shorter durations: <21 days in the rat<sup>10,11</sup> and 6 weeks in the mouse.<sup>12,13</sup> For these models, both interanimal variability and variability in the magnitude of elevations are limiting factors, necessitating relatively large numbers of experimental cohorts.<sup>5</sup> In contrast, cauterization of two or three episcleral veins alone elevates IOP by reducing venous outflow, thereby increasing aqueous fluid pressure.<sup>8,14–17</sup> Although relatively consistent between animals, the potential for ocular ischemia and neovascularization can confound interpretation of this model.<sup>5,9</sup> These most widely used models are limited by the absence of a repeatable internal control in which an equivalent insult in the fellow eye would not result in extended elevated IOP. Such a control would allow the assessment of IOP-induced pathology without confounding factors, such as injury induced by the surgical procedure (e.g., vessel cauterization and sclerosis). Although the potential for uncontrolled confounds is well recognized, there have been few alternatives. Additional rodent systems for ocular hypertension are also available but have been less extensively used. These include ligation of extraocular veins<sup>18</sup> and intra-aqueous injection of hyaluronic acid.<sup>19</sup>

We sought to establish a rodent model of ocular hypertension in which both IOP magnitude and duration could be manipulated relatively simply with minimal confounding factors and with an internal control for each animal. Here we describe a procedure for injecting small volumes of polysty-

rene microbeads into the anterior chamber to impede aqueous outflow and elevate IOP. This model builds on a limited number of earlier studies using microbeads to elevate IOP in primates,<sup>20</sup> rats,<sup>21</sup> and rabbits.<sup>22</sup> For each animal, one eye is injected with microbeads and other is injected with an equivalent volume of saline. For maximal usefulness as a rodent model, we demonstrate our procedure for use in both rats (2.5- to 7- $\mu$ L injections) and mice (1- $\mu$ L injections). We show that IOP after microbead injection is highly consistent both in duration and magnitude with interanimal variability approximately 5% of the mean, whereas saline injection affected IOP very little regardless of volume and duration. Overall, the flexibility and consistency of this model, with a simple internal control, affords the opportunity for specific assessment of IOP-induced pathology.

## MATERIALS AND METHODS

### Animals

This study was conducted in accordance with regulations set forth in the ARVO Statement for the Use of Animals in Ophthalmic and Vision Research. Animal protocols were approved by the Institutional Animal Care and Use Committee of the Vanderbilt University Medical Center. Male Brown Norway rats aged 3 to 7 months were obtained from Charles River Laboratories (Wilmington, MA) and individually housed for the duration of the experiments. Male C57BL/6 mice aged 3 to 7 months were obtained from Jackson Laboratories (Bar Harbor, ME) and housed in groups for the duration of the experiments.

### Microbead Surgeries

For microbead surgeries, one eye was injected with sterile 15- $\mu$ m polystyrene microbeads, conjugated to Alexa Fluor 488 chromophore, in a  $1 \times 10^6$  microbeads/mL solution (Molecular Probes, Eugene, OR), and the other eye was injected with an equivalent volume of sterile physiologic saline (Fisher Scientific, Fair Lawn, NJ). As such, each animal serves as its own control. We selected 15- $\mu$ m-diameter microbeads based on pilot studies in our laboratory evaluating 5- to 15- $\mu$ m microbeads alone and in combination (data not shown). Before injections, animals were anesthetized with isoflurane (Minrad Inc., Bethlehem, PA), which was controlled by a pump that allows continuous administration for up to 12 hours. Pupils were dilated with 1% tropicamide ophthalmic solution (Bausch & Lomb, Tampa, FL), and anesthetic drops (0.5% proparacaine hydrochloride; Bausch & Lomb) were applied to each eye. We pulled micropipettes from borosilicate glass capillaries (1.0/0.75 mm OD/ID with filament; World Precision Instruments, Sarasota, FL) to a final diameter of approximately 100  $\mu$ m on a horizontal electrode puller (model P-97; Sutter Instruments Co., Novato, CA). For injections, we used a manual microsyringe pump (DMP; World Precision Instruments) equipped with an injection assembly (MMP-KIT; World Precision Instruments). The glass micropipette fit directly into the injection assembly, which was connected to the microsyringe pump by polyethylene tubing. Mineral oil was used to fill the injection apparatus, and the aqueous-oil interface was visually examined after each injection to confirm injection of the appropriate volume. After dilation of the iris and protraction of the eye with forceps, a micromanipulator was used to position the micropipette above the anterior chamber approximately 3 mm central to the ora serrata. The slope of the micropipette was closely monitored to avoid contact with the lens and to ensure proper filling of the anterior chamber. For rats, 2.5- $\mu$ L, 5- $\mu$ L, or 7- $\mu$ L injection volumes (approximately 2500, 5000, or 7000 microbeads, respectively) were used. For mice, a 1- $\mu$ L injection volume (approximately 1000 microbeads) was used. The rate of injection (1  $\mu$ L/s) was controlled by the experimenter and remained constant between subjects. After injection, antibiotic drops (0.5% moxifloxacin hydrochloride ophthalmic solution; Alcon, Fort Worth, TX) were placed on each eye, and the animal was allowed to recover for 24 hours before resumption of IOP measurements.

### IOP Measurements: Rat

To avoid the health risks associated with daily administration of anesthesia and the IOP-lowering effect of anesthetic agents,<sup>23</sup> IOP measurements were performed in awake rats. To allow accurate and humane measurement of IOP in awake rats, we used a behavioral training paradigm that began approximately 2 weeks before experiments.

**Behavioral Training Paradigm.** Rats were handled for 1 week before the initiation of training. For the first phase of training, rats were acclimated to the application of anesthetic drops (0.5% tetracaine), tactile contact with each eye, and the alert signals of the tonometer (Tono-Pen; Reichert, Inc., Depew, NY). In the second phase of training, generalized tactile contact with each eye was replaced with actual tonometer contact followed by actual tonometer measurements. The latency between initiation of training and full tonometer measurements was between 5 and 10 days.

**IOP Measurements.** The tonometer was used with a protective thin rubber sheath over the exposed metal sensor. IOP for each eye was determined as the mean of 25 to 30 tonometer readings. Baseline IOP readings were recorded for two consecutive days before polystyrene microbead/saline injections. The first experimental IOP readings were obtained 24 hours after injection surgery. IOP readings were then obtained daily until termination of the experiment. To avoid irritation of the cornea, saline eye drops were administered daily to each eye at the completion of IOP measurements.

IOP was measured for different lengths of time in cohorts of rats so that we could harvest tissue for other purposes. All IOPs for each animal are reported; no animal was excluded from our analysis because IOP did not remain elevated. For single 2.5- $\mu$ L injections, IOP measurements for individual rats ranged from 3 to 6 days ( $n = 5$ ) to 2 weeks ( $n = 4$ ) after injection. For single 5- $\mu$ L injections, measurements ranged from 6 days ( $n = 7$ ) to 13 days ( $n = 4$ ); for single 7- $\mu$ L injections, measurements were taken for 10 days in four animals. A cohort of seven rats had IOP measured daily until day 20 for a single 5- $\mu$ L injection. Finally, a cohort of 11 rats had two 5- $\mu$ L injections; the second occurring 14 to 17 days after the first. IOP was measured in this cohort for 5 to 8 weeks.

### IOP Measurements: Mouse

IOP measurements in mice were performed as previously described with some modification.<sup>24-26</sup> To avoid agitation and because behavioral training proved difficult given the lack of docility, IOP was measured in an anesthetized, rather than an awake, behaving state. As with the rats, the tonometer (Tono-Pen; Reichert, Inc.) was used with the protective sheath over the sensor. Briefly, mice were anesthetized with an isoflurane pump before measurement of IOP. IOP for each eye was determined as the mean of 25 tonometer measurements. To avoid irritation of the cornea, hydrating eyedrops were administered daily to each eye at the completion of IOP measurements.

Cohorts of mice also had IOPs measured for different lengths of time. As for the rats in our study, all IOPs for each animal are reported with no animal excluded because IOP did not remain elevated. All mice reported had a single 1- $\mu$ L injection and IOP measurements ranging from 2 weeks ( $n = 1$ ) to 4 weeks ( $n = 5$ ).

### Tissue Procurement

At the conclusion of the experiments, subjects were administered an overdose of pentobarbital (200 mg/kg; Hospira, Inc., Lake Forest, IL) and were killed by transcardial perfusion with 4% paraformaldehyde (Sigma, St. Louis, MO). Whole eyes were dissected from the head and postfixed as necessary.

### Histopathology

For assessment of microspheres in the anterior segment, fluorescence in whole mount preparations of anterior segment were examined with a digitally interfaced, upright microscope equipped with four fluorescent cubes (Olympus, Melville, NY) and fluorescent confocal micros-

copy (Olympus) at the Vanderbilt University Cell Imaging Core. For quantification of axonal populations in the optic nerve, we followed a protocol as described in recent work.<sup>26</sup> Briefly, a 2- to 3-mm section of optic nerve proximal to the globe was isolated, postfixed for 1 hour in 4% paraformaldehyde, and prepared for embedding and semithin sectioning, as previously described.<sup>25</sup> Using 100 $\times$  oil-immersion and differential interference contrast optics, photomicrographs of each section were collected as a montage with a microscope containing a motorized X-Y-Z stage and a digital charge-coupled device video camera (Provis AX70; Olympus). Each montage was contrast- and edge-enhanced using macro-routines written with a software package (ImagePro; Media Cybernetics, Silver Spring, MD). An additional routine was used to identify and count each axon in the montage for which a myelin sheath could be identified. We used this information to calculate the mean local axon density for each section of nerve.

### Statistical Analysis

Analysis was aided by statistical analysis software (Systat 12; Systat Software, Inc., Chicago, IL). For comparisons of means for samples meeting normality criteria, standard parametric statistics were used (Student's *t*-test, ANOVA *F*-statistic). For samples failing normality, nonparametric rank statistics were used (Mann-Whitney *U* test, Kruskal-Wallis *H*-statistic). For testing whether the slope of a best-fitting regression line differed from zero and whether two slopes differed, we used the Fisher *F*-ratio calculated from the least-squares regression. For all cases, only the *P* value for the corresponding test was indicated for simplicity. The use of additional statistics is explained in the text as needed.

## RESULTS

### Microbead-Induced Elevations in IOP of the Rat Eye

After dilation of the iris, protraction of the eye with forceps and injection (Figures 1A), fluorescent microbeads were widely distributed throughout the aqueous regardless of injection volume and could be seen moving with the flow of aqueous (Fig. 1B). Within 30 minutes, fewer microbeads were visible, but they were clustered near the trabecular meshwork region of the anterior chamber (Fig. 1C). To determine whether these microbeads were present near aqueous outflow channels, we used fluorescence microscopy to examine histologic preparations from rat eyes. Clusters of microbeads were observed in the connective tissue of the iridocorneal angle of a flat-mount preparation of the anterior segment (Fig. 1D, left). In vertical sections through the anterior segment, microbeads cluster near the iridocorneal angle (Fig. 1D, right). These observations show that microbeads are carried with the aqueous humor toward the trabecular meshwork.

To determine how different volumes of microbeads influence IOP in rats, we injected 2.5  $\mu$ L, 5  $\mu$ L, or 7  $\mu$ L saline or microbeads and monitored IOP from 1 to 2 weeks, generally three to five times per week. Figure 2A depicts the daily IOP measurement for individual animals receiving each injection volume. For saline-injected eyes, IOP fluctuated about a consistent baseline value of approximately 21 mm Hg, whereas microbead injection induced an increase of 30% to 40% (Fig. 2A). Figure 2A also demonstrates that for some animals receiving either 2.5 or 5  $\mu$ L injections, microbead injection elicited a rapid (1 day after injection) elevation in IOP that abated by 7% to 8% for 1 to 2 days before recovering.

The mean IOP for the saline eyes across animals and days did not depend on injection volume (Fig. 2B, mean  $\pm$  SD): 21.4  $\pm$  0.95 mm Hg for 2.5- $\mu$ L, 21.3  $\pm$  1.3 mm Hg for 5- $\mu$ L, and 21.3  $\pm$  0.96 mm Hg for 7- $\mu$ L injections (*P* = 0.34). For these data, each SD was approximately 5% of the mean; hence, the interday variability was modest for each injection volume. The

postinjection IOP in microbead-injected eyes averaged across days tended to increase with injection volume (Fig. 2B; bracketed period): 26.9  $\pm$  1.7 mm Hg for 2.5- $\mu$ L, 28.8  $\pm$  1.6 mm Hg for 5- $\mu$ L, and 29.7  $\pm$  1.2 mm Hg for 7- $\mu$ L injections. The increase in mean IOP from 2.5 to 5  $\mu$ L and from 2.5 to 7  $\mu$ L were both highly significant (*P* < 0.001), whereas the elevated IOPs for 5 and 7  $\mu$ L did not differ (*P* = 0.07). As with the saline eyes, each SD for the postinjection means was modest (4%–6% of the mean), indicating a highly regular elevation in IOP. That the mean IOP increased with injection volume for the microbead eyes but not for the saline-injected eyes suggested that the increase was the result of the number of actual microbeads rather than fluid volume, as calculated (see Materials and Methods).

Figure 2 shows that each microbead injection volume was efficacious in elevating IOP above that for the saline eyes, and indeed each postinjection mean elevation was significant (*P* < 0.001 for each volume). However, it is apparent from Figure 2A that the interanimal variability decreased with increasing injection volume, so that the 2.5- $\mu$ L rats demonstrated the largest spread in IOP between individuals on a given day, whereas the 7- $\mu$ L rats demonstrated the smallest spread in IOP. Thus, in calculating the mean postinjection IOP for the microbead eye across animals for a given day (Fig. 2B), the average daily SD decreased from 2.1 for 2.5- $\mu$ L to 1.7 for 5- $\mu$ L to 1.2 for 7- $\mu$ L injections (4%; *P* = 0.006). These correspond to 8%, 6%, and 4% of the mean postinjection IOP, respectively. This change is apparent in the diminishing magnitude of the error bars with increasing microbead injection volume in Figure 2B. For 7  $\mu$ L, certainly the smaller size of the cohort could contribute to less variability.

We then calculated the difference in mean IOP between the saline- and microbead-injected eyes over time by subtracting the data shown in Figure 2B. As suggested in Figure 2, the magnitude of this difference (i.e., the IOP elevation) was dependent on injection volume (Fig. 3A). For 2.5- $\mu$ L-injected animals, the mean difference in postinjection IOP between microbead and saline eyes was 4.4  $\pm$  1.3 mm Hg. For the 5- $\mu$ L-injected animals, this difference increased significantly to 7.2  $\pm$  0.8 mm Hg (*P* < 0.001). For the 7- $\mu$ L-injected animals, the difference was 7.5  $\pm$  1.0 mm Hg, which was statistically different from the 2.5- $\mu$ L difference (*P* < 0.001) but not from the 5- $\mu$ L difference (*P* = 0.42). For 5  $\mu$ L, the difference in IOP between the saline- and microbead-injected eyes for the postinjection period had a best-fitting regression line whose slope was not different from zero (*P* = 0.58).

The difference curves in Figure 3A demonstrate that after injection, IOP elevation remained relatively stable compared with the saline eye over this short experimental period. As such, the cumulative exposure to elevated IOP should increase roughly linearly with time.<sup>27</sup> To test this directly, we calculated the cumulative area under the difference curves in Figure 3A as a function of time in units of millimeter of mercury per days (Fig. 3B). As expected, the cumulative exposure to pressure increased nearly monotonically for each injection volume. To test this, we determined the best-fitting multiparameter sigmoidal function and compared the goodness-of-fit with that of the best-fitting regression line for the 2.5- $\mu$ L and 5- $\mu$ L cumulative pressure data sets, both of which had several more data points than the 7- $\mu$ L set. The best-fitting sigmoids are shown in Figure 3B. For the 2.5- $\mu$ L data, the sigmoidal function provided a significantly improved prediction of the data over the best-fitting line (Fisher *F* ratio = 3.7; *P* = 0.02). In contrast, for the 5- $\mu$ L data, the best-fitting sigmoid approached a straight line and in fact was not different from the regression line (Fisher *F* ratio = 0.32; *P* = 0.95). The rate of pressure accumulation for the 5- $\mu$ L injection was also significantly higher than the 2.5- $\mu$ L injection (slope of 7.1 vs. 5.3; *P* < 0.001).

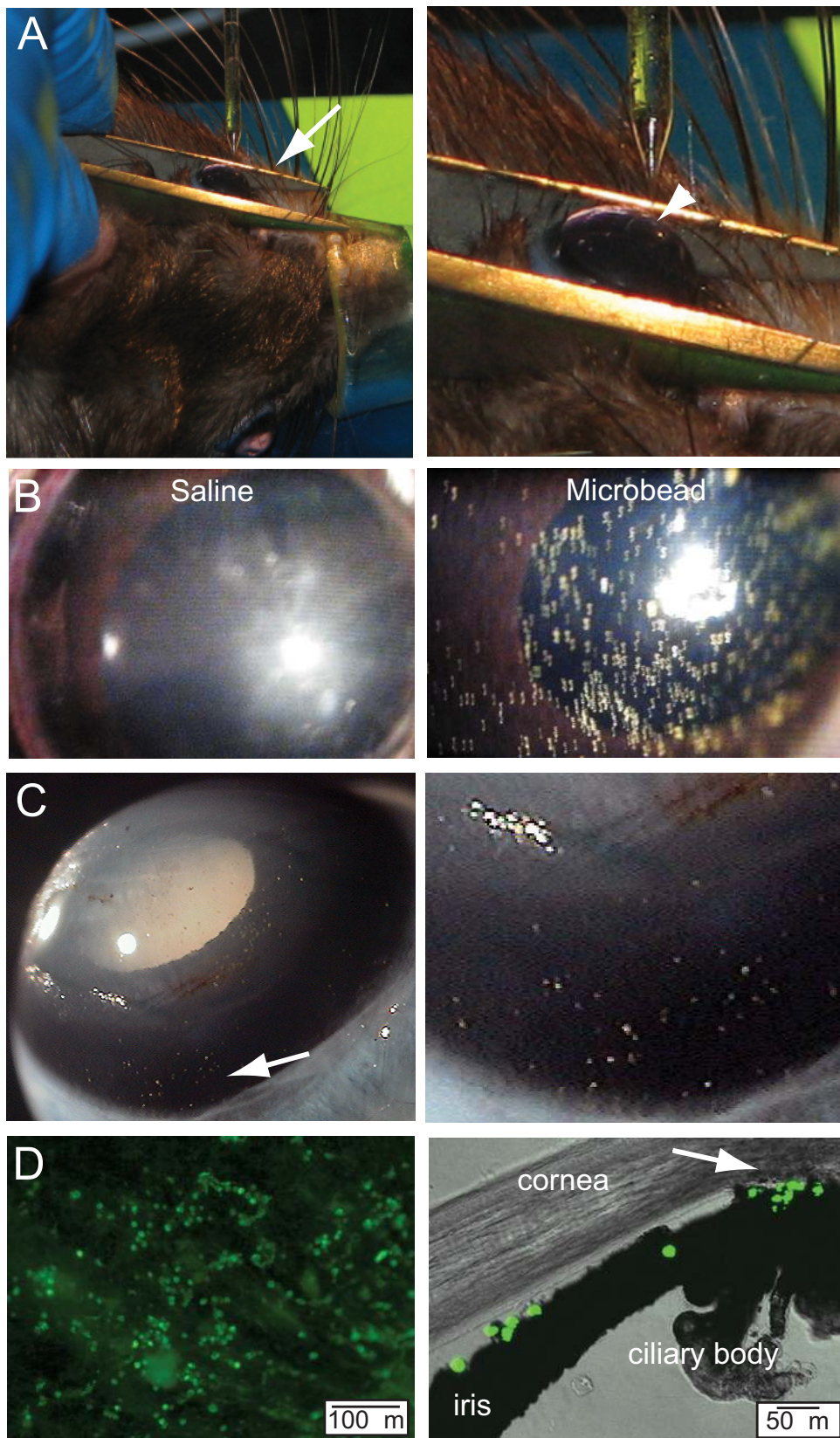


**FIGURE 1.** Injection of microbeads into the anterior chambers of rats. (A) Microbead injection into the anterior chamber of a rat eye using a glass micropipette (approximately 100- $\mu$ m diameter; *arrowhead*) with forceps (*arrow*) to retract the eyelid and stabilize the eye. Low- and high-magnification views included. (B) Photomicrographs of the anterior segment immediately after injection with 5  $\mu$ L saline (*left*) or 5  $\mu$ L microbeads (*right*). Microbeads are apparent in the aqueous with no evidence of overt trauma to cornea or iris. (C) Microbead-injected eye 30 minutes after 5  $\mu$ L injection (*left*). Microbeads localize in the posterior region of the anterior segment toward the area of aqueous outflow (*arrow*, magnified in the *right*). (D) Confocal fluorescence micrograph of flat-mounted anterior chamber from an eye injected with 5  $\mu$ L microbeads (*left*). Location is near the trabecular meshwork around the iridocorneal angle. In vertical section (*right*), microbeads are apparent in the iridocorneal angle and cluster near the point of aqueous outflow (*arrow*).

Given that the 5- $\mu$ L injection seemed to yield the most consistent elevation in IOP, we determined next how long a single microbead injection would elevate IOP. Figure 3C demonstrates the mean daily IOP averaged across a cohort of seven

rats followed until day 20. As earlier, postinjection IOP remained stable to approximately day 13. Although there appeared to be a slight downward trend, the slope of the best-fitting regression line for this period was not significantly

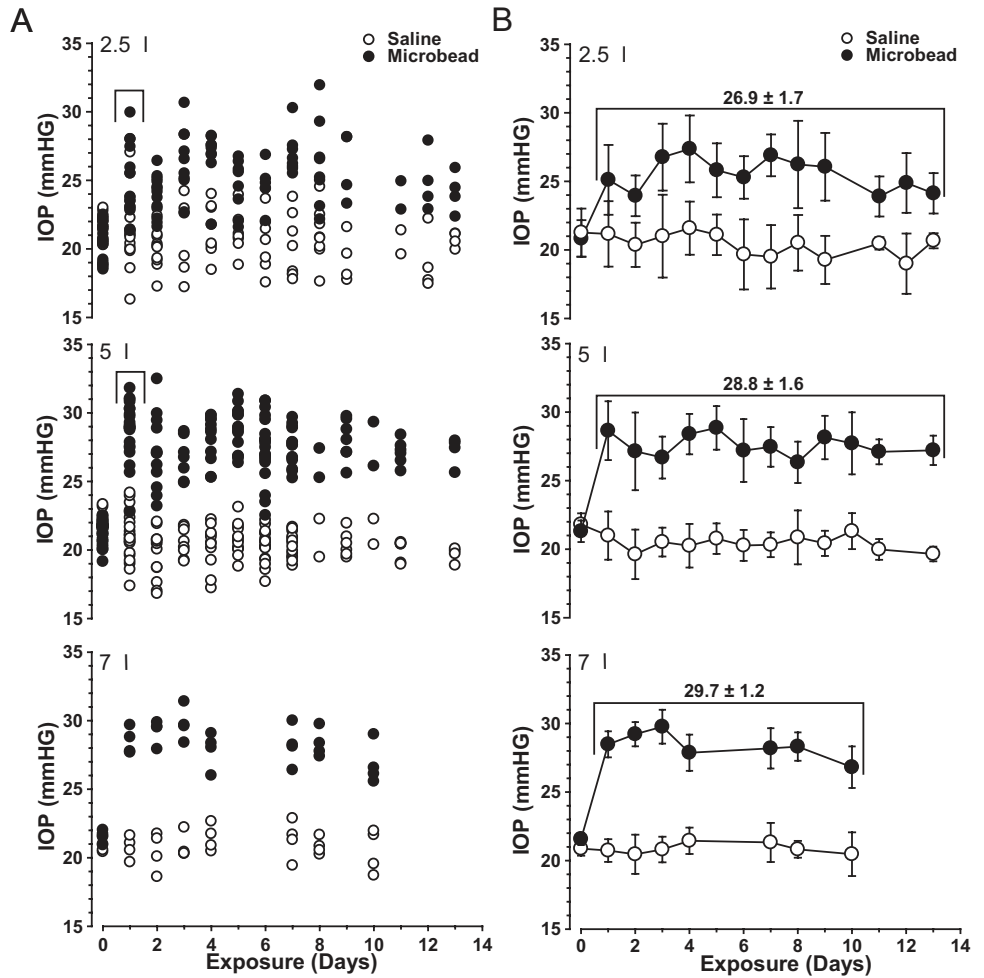


**FIGURE 2.** Injection volume determines magnitude of IOP elevation in rats. **(A)** Daily IOP measurements for individual rats receiving a single 2.5  $\mu\text{L}$  ( $n = 15$ ), 5  $\mu\text{L}$  ( $n = 21$ ), or 7  $\mu\text{L}$  ( $n = 4$ ) unilateral injection of microbeads (filled circles) and an equivalent volume of saline (open circles) in the opposing eye. IOP is plotted as a function of time, where day 0 is before injection and day 1 is 24 hours after injection. IOP was monitored for 3 to 13 days (2.5- $\mu\text{L}$  injections), 6 days to 2 weeks (5  $\mu\text{L}$ ), or 10 days (7  $\mu\text{L}$ ). Brackets indicate increase in IOP 1 day after injection for 2.5- $\mu\text{L}$  and 5- $\mu\text{L}$  bead injections, followed by a transient decline. **(B)** IOP averaged across the cohort injected once with 2.5  $\mu\text{L}$ , 5  $\mu\text{L}$ , or 7  $\mu\text{L}$  microbeads in the test eye (filled circles) and equivalent volume of saline in the other eye (open circles). Brackets indicate postinjection period with corresponding mean  $\pm$  SD.

different from zero ( $P = 0.17$ ). However, after this point, IOP in the microbead eyes began to decrease, falling by more 2.5 mm Hg by day 20. This was a significant decline from the postinjection period through day 13 ( $P = 0.05$ ), indicating that the first sign of IOP recovery from a single 5- $\mu\text{L}$  injection can occur at about 2 weeks.

### Extension of IOP Elevation in the Rat

Next we sought to determine whether IOP elevation could be extended by a subsequent injection of 5  $\mu\text{L}$ . As earlier, the control eye received an equivalent volume of saline. For each animal in a cohort of 11, IOP from an initial 5- $\mu\text{L}$  injection was followed to 13 days, with a second injection given between days 14 and 17. This point was chosen based on the data in Figure 3C, which indicated IOP began to drop approximately 2 weeks after the first injection. IOP was then followed in most of the animals for an additional 20 to 23 days, for a total period of just more than 5 weeks. IOP was followed in a small subset of the animals for nearly 8 weeks. Individual animal IOPs are shown in Figure 4A for the entire experimental period.

IOP was highly regular between the two injections (Fig. 4B). For the saline eye, mean IOP after the second injection ( $21.1 \pm 0.8$  mm Hg) was the same as that for the first ( $21.0 \pm 0.5$  mm Hg;  $P = 0.89$ ). For the microbead eye, mean IOP after injection for the second injection was also similar to the first:  $28.2 \pm 0.8$  mm Hg versus  $28.5 \pm 0.7$  mm Hg ( $P = 0.25$ ). The slopes of the best-fitting regression lines did not differ for the two postinjection periods for the microbead eyes ( $P \geq 0.60$ ), indicating similarity in IOP elevation. In addition, the regres-

sion lines for the entire 8-week period for both the saline and the microbead IOPs had slopes that did not differ from zero ( $P \geq 0.66$ ). Thus, a second injection of equal volume could extend the IOP elevation by an additional 3 to 6 weeks without a significant change in the magnitude of elevation.

The constancy in IOP between the first and second microbead injections is illustrated explicitly in Figure 4C, which shows the difference in daily mean IOP between the microbead- and saline-injected eyes. For the second injection, the postinjection difference was  $7.5 \pm 0.2$  mm Hg compared with  $7.3 \pm 0.3$  mm Hg for the first ( $P = 0.35$ ). Cumulative exposure to elevated IOP in millimeters of mercury per days for the entire injection period increased monotonically (Fig. 4D). The goodness-of-fit for the best-fitting multiparameter sigmoidal function was not significantly improved from that for the best-fitting regression line (Fisher  $F$  ratio = 0.42;  $P = 0.80$ ). The latter had a rate of accumulation of 7.6 mm Hg/d, very close to the rate of 7.1 mm Hg/d for the single 5- $\mu\text{L}$  injection shown in Figure 3B. These data indicate that though the elevation in IOP afforded by a second 5- $\mu\text{L}$  injection was similar in magnitude to that elicited by a single injection, the period of elevation was much longer—up to 6 additional weeks.

### Microbead-Induced IOP Elevations in Mouse Eyes

Next, we examined whether a 1- $\mu\text{L}$  microbead injection could elevate IOP in C57BL/6 mice. We chose this volume based on the size difference between the anterior chambers of rats and

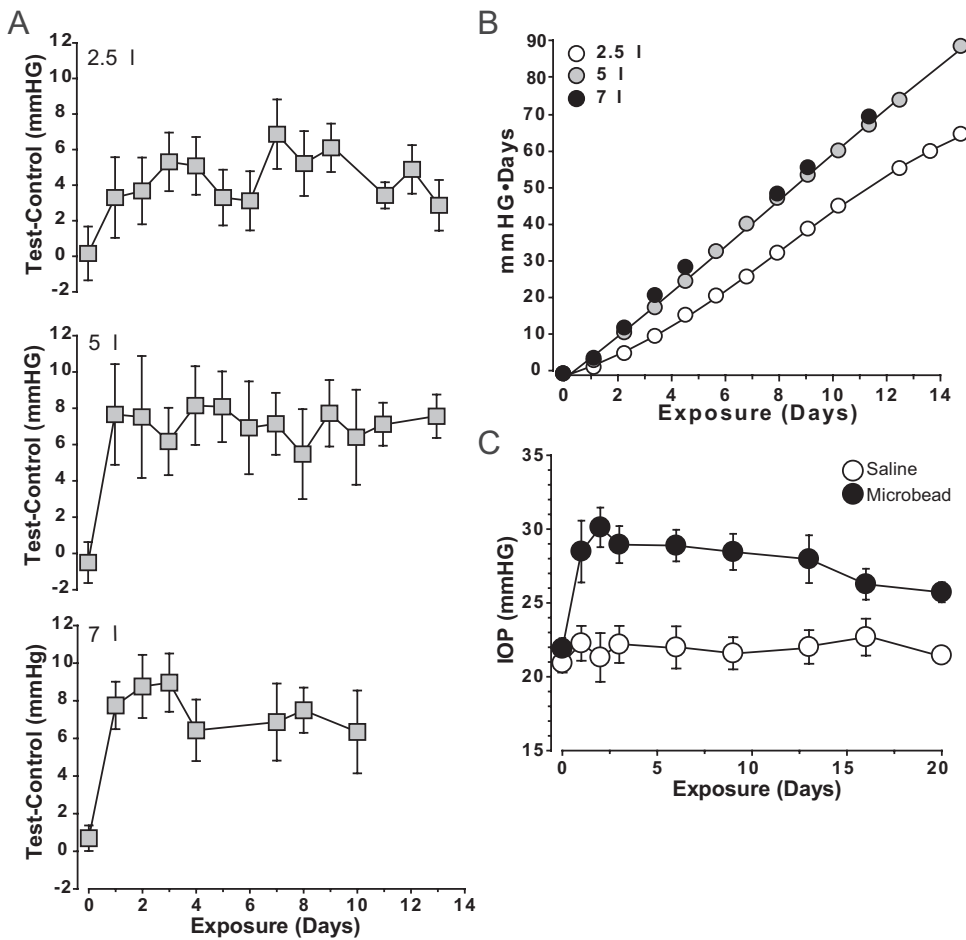


**FIGURE 3.** Injection volume and pressure exposure over time in rats. (A) Difference in mean IOP between microbead- and saline-injected rat eyes (test-control) after a single 2.5- $\mu$ L, 5- $\mu$ L, or 7- $\mu$ L injection plotted against exposure time, where day 0 is before injection and day 1 is 24 hours after injection. (B) Cumulative exposure to elevated IOP over time (millimeters of mercury per day) calculated from the difference curves in (A) for a 2.5- $\mu$ L (white circles), 5- $\mu$ L (gray circles), or 7- $\mu$ L (black circles) injection. Lines represent best-fitting multiparameter sigmoidal functions for the 2.5- $\mu$ L and 5- $\mu$ L data. (C) Daily IOP averaged across a cohort of seven rats receiving a single 5- $\mu$ L injection of microbeads (filled circles) and equivalent volume of saline in opposing eye (open circles); measurements taken until day 20 after injection for each animal. Data represent mean  $\pm$  SD.

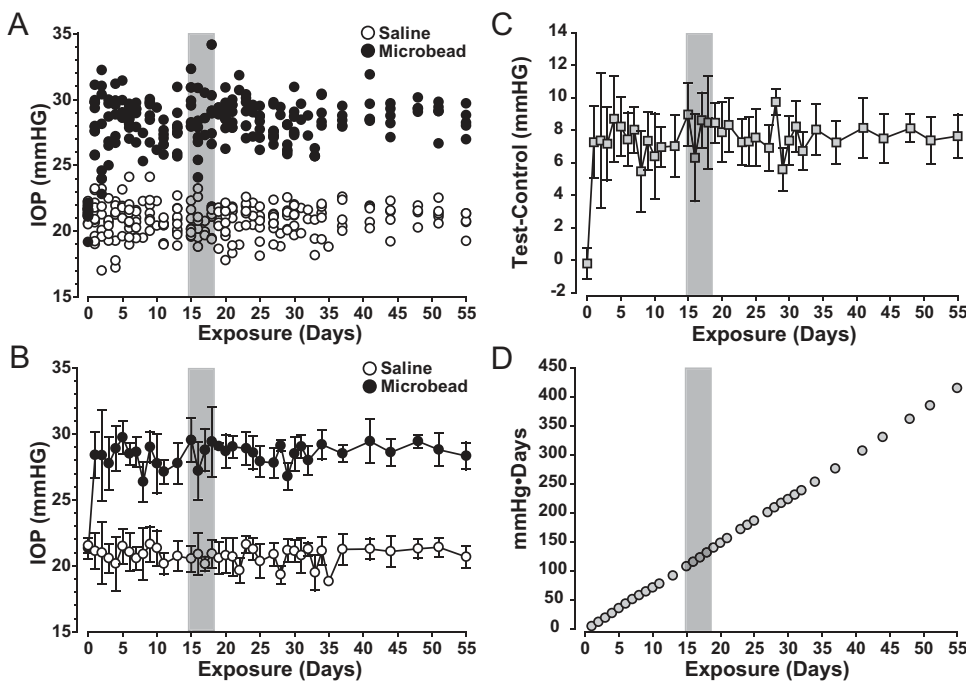
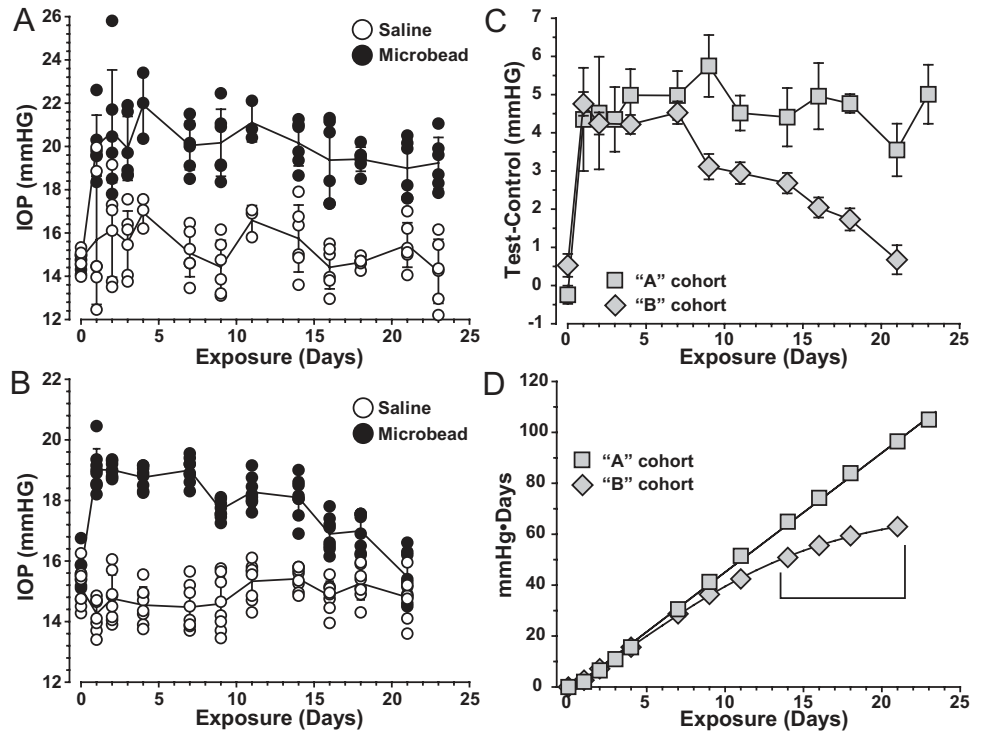


**FIGURE 4.** Second injection of 5  $\mu$ L extends IOP elevation in rats. (A, top) Daily IOP measurements for individual rats ( $n = 11$ ) with two 5- $\mu$ L unilateral injections of microbeads (filled circles) and an equivalent volume of saline (open circles) in the opposing eye. Day 0 is before injection and day 1 is 24 hours after the first injection. Each animal received the second injection 14 to 17 days after the first. Seven of the animals were followed to approximately 5 weeks, and the rest were monitored to nearly 8 weeks. (B) Mean daily IOP across the cohort for first and second injections. (C) Difference in mean IOP between the microbead and saline eyes (test-control) for the entire experimental period. (D) Cumulative exposure to elevated IOP over time (mm Hg per day) calculated from the difference curves in C for dual 5- $\mu$ L injections. For all panels, the period containing the second injection (14–17 days) is indicated (shaded region).

**FIGURE 5.** Single injection of 1  $\mu\text{L}$  elevates IOP in mice. (A) Daily IOP measurements for individual mice ( $n = 6$ ) after a single 1- $\mu\text{L}$  unilateral injection of microbeads (filled circles) and an equivalent volume of saline (open circles) in the opposing eye. Eyes were monitored for 23 days after injection without a significant decrease in IOP. Day 0 is before injection and day 1 is 24 hours after injection. Line represents IOP averaged across the cohort (mean  $\pm$  SD). (B) A second cohort of mice ( $n = 8$ ) with same injection regimen as in (A) but with a different experimenter. IOP returned to baseline by day 21. (C) Difference in mean IOP between microbead- and saline-injected mouse eyes (test-control) for the cohorts shown in (A) and (B) plotted against exposure time. (D) Cumulative exposure to elevated IOP over time (mm Hg per day) calculated from the difference curves in (C) with best-fitting multiparameter sigmoidal function (solid lines). Bracket indicates period without additional accumulation for the cohort in (B).



mice. In rats, the volume of the anterior chamber is approximately 15  $\mu\text{L}$ <sup>28</sup> compared with 7  $\mu\text{L}$  in mice.<sup>29</sup> IOP was measured every 1 day to 2 days, as described, for 23 days for one cohort ( $n = 6$ ; Fig. 5A) and for 21 days for a second cohort ( $n = 8$ ; Fig. 5B). Injections for the second cohort were performed by a less experienced user.

For the first cohort (Fig. 5A), IOP for the saline eye fluctuated about a baseline value of approximately 15 mm Hg ( $15.3 \pm 0.80$  mm Hg). Microbead injection induced an increase of approximately 30% ( $20.0 \pm 0.8$  mm Hg), a significant elevation ( $P \ll 0.001$ ). Both sets of measurements were approximately 25% lower than for rats, some of which could be attributable to our use of isoflurane anesthesia. As seen in rats (Fig. 2), each SD across days for both the saline and the microbead IOPs was approximately 5% of the mean; hence, the interday variability was modest, indicating a highly regular elevation in IOP. The interanimal variability also was modest. In calculating the mean IOP for the microbead eye across animals for a given day, the average daily SD after injection was 1.3 mm Hg (approximately 7.5% of the mean), which was the same for the saline eye.

For the second cohort of mice (Fig. 5B), the IOP for the saline eye was similar to that for the first cohort:  $14.9 \pm 0.40$  mm Hg. However, the IOP elevation for the microbead eye was significantly lower:  $17.9 \pm 1.1$  mm Hg ( $P < 0.001$ ). This was due in part to a lesser peak value of approximately 19 mm Hg compared with 21 to 22 mm Hg for the first cohort. However, IOP elevation in the microbead eye also decreased relatively rapidly, returning to the saline eye values by day 21 ( $P = 0.10$ ). For the first cohort (Fig. 5A), the difference in postinjection IOP between microbead and saline eyes was  $4.6 \pm 0.6$  mm Hg and was nearly flat across days (Fig. 5C). The slope of the best-fitting regression line for the postinjection period was not significantly different from zero ( $P = 0.31$ ). For the second cohort, in contrast, the difference curve was flat only until day 7, at which point it decreased until reaching a value close to 0 by day 21.

The best-fitting multiparameter sigmoidal function for the cumulative pressure exposure for the first cohort (Fig. 5A) was

not significantly different from the best-fitting regression line ( $P = 0.24$ ; Fig. 5D). For this line, the rate of pressure accumulation was 4.7 mm Hg/d ( $P \ll 0.001$ ). For the second cohort (Fig. 5B), the sigmoidal function provided a significantly improved representation of the data over the best-fitting line (Fisher  $F$  ratio = 4.8;  $P = 0.008$ ). This was apparent especially for latter times for which accumulation did not change (Fig. 5D, bracketed area). Thus, though a single 1- $\mu\text{L}$  injection of microbeads in the mouse can elevate IOP above baseline for more than 3 weeks, variability was seen in the duration of IOP elevation between the two cohorts.

### Pathology in the Optic Nerve Resulting from Microbead-Induced IOP Elevation

Axonal degeneration in the optic nerve is an important hallmark for models of glaucoma involving increased IOP.<sup>4-7</sup> To ascertain whether elevations due to microbead injection similarly induce optic nerve abnormalities, we prepared cross-sections through the optic nerves of both rats and mice and quantified mean axon density and number of axons. Figure 6A shows examples of nerves from the saline-injected right eye (left) and microbead-injected left eye (right) for the cohort of rats we monitored until approximately 5 weeks after receiving a second 5- $\mu\text{L}$  injection 14 to 17 days after the first (Fig. 4A, IOP). The nerve from the microbead eye demonstrates clear axonal disorder, reduction in axon packing, and axonal distension. Figure 6B shows similar examples from the mice receiving a single 1- $\mu\text{L}$  injection with elevated IOPs for approximately 4 weeks (Fig. 5).

For the rat cohort, average axon density in nerves from the saline/right eyes ( $3.7 \pm 0.1 \times 10^5$  axons/ $\text{mm}^2$ ) was the same as naive nerves ( $3.6 \pm 0.2 \times 10^5$  axons/ $\text{mm}^2$ ;  $P = 0.85$ ), whereas axon density in nerves from the microbead/left eyes was 16% lower ( $3.1 \pm 0.2 \times 10^5$  axons/ $\text{mm}^2$ ;  $P = 0.04$ ). For mice, average axon density in the saline nerves ( $4.4 \pm 0.2 \times 10^5$  axons/ $\text{mm}^2$ ) did not differ from that of naive nerves ( $4.2 \pm 0.2 \times 10^5$  axons/ $\text{mm}^2$ ;  $P = 0.53$ ), whereas axon density in the microbead nerves was 27% lower ( $3.2 \pm 0.2 \times 10^5$  axons/

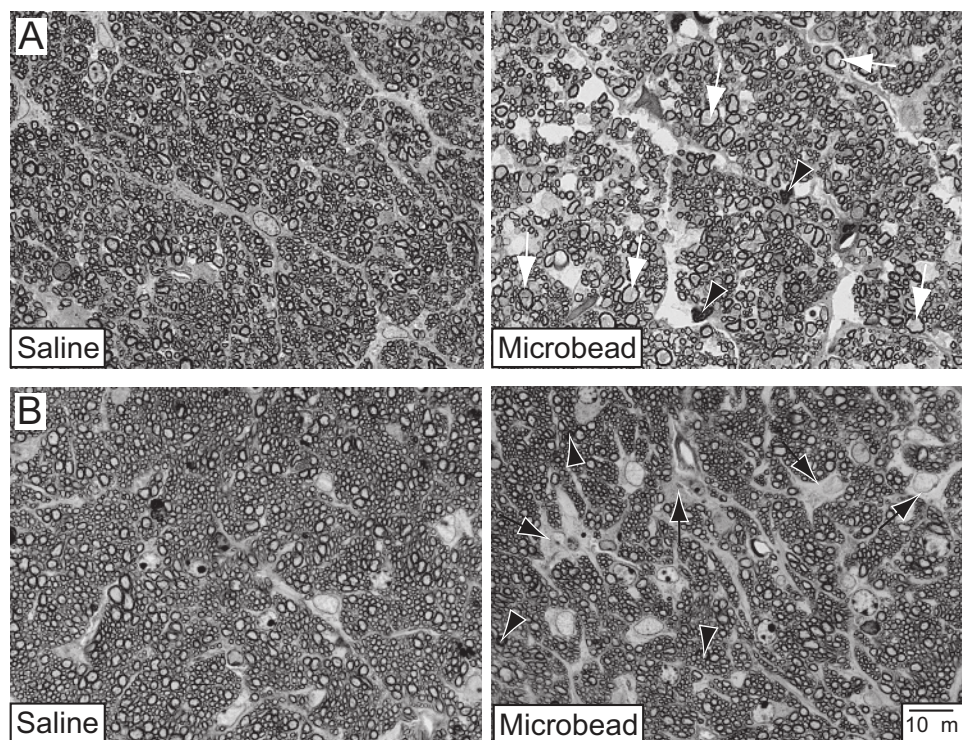
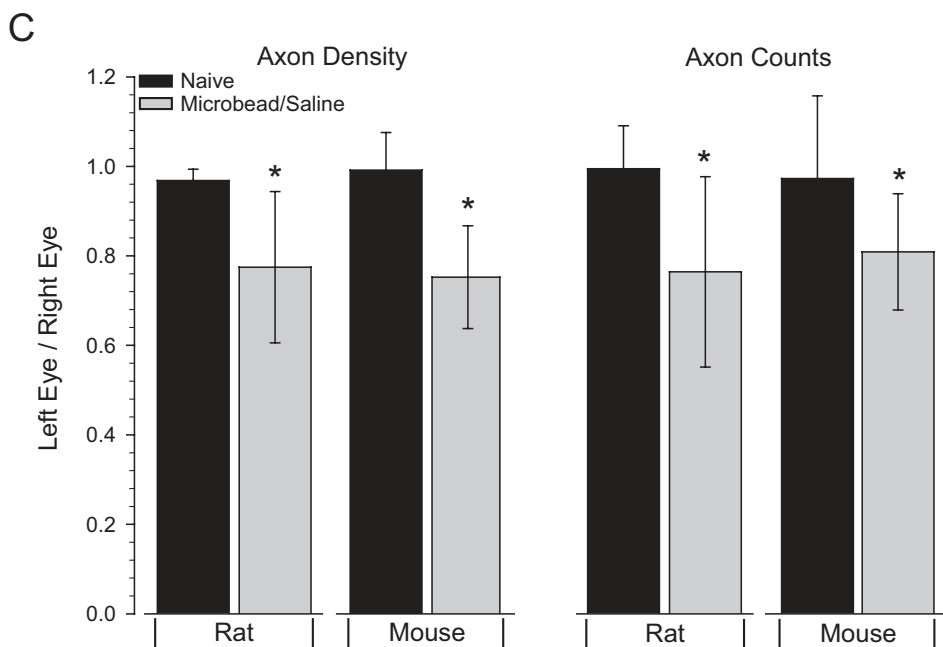


**FIGURE 6.** Optic nerve abnormality resulting from microbead-induced elevations in IOP. **(A)** High-magnification light micrographs of cross-sections through rat optic nerve after dual 5- $\mu$ L injections of saline (*left*) or microbeads (*right*). Second injection occurred 2 weeks after the first; tissue was harvested 22 days later. IOPs are shown in Figure 4E. Nerve of bead-injected eye shows diminished axon density, enlarged axons (*white arrows*), and degenerating axon profiles (*black arrowheads*). **(B)** Cross-sections through mouse optic nerve after a single 1- $\mu$ L injection of saline (*left*) or microbeads (*right*). Tissue was harvested 28 days after injection; IOPs are shown in Figure 5A. Nerve from microbead eye shows diminished axon density, glial hypertrophy (*black arrows*), and degenerating profiles (*black arrowheads*). Scale applies to all micrographs. **(C)** Mean axon density and total number of axons for optic nerves from naive, saline-injected (right eye) and microbead-injected (left eye) rats and mice, shown as ratios of left to right eyes. *Asterisks* indicate a significant difference between saline- and microbead-injected nerves for both rat (15% decrease, dual 5- $\mu$ L injections) and mice (23% decrease, single 1- $\mu$ L injection). IOPs of rat cohort are shown in Figure 4E; those of the mouse are shown in Figure 5A.



mm<sup>2</sup>;  $P = 0.03$ ). We also calculated the total number of axons in the nerves by multiplying axon density by the cross-sectional nerve area. As with axon density, the average number of axons in rat nerves from saline eyes ( $8.9 \pm 0.4 \times 10^4$  axons) was the same as in naive nerves ( $9.4 \pm 0.4 \times 10^4$  axons;  $P = 0.53$ ), whereas the number of axons in microbead nerves was 20% lower ( $7.1 \pm 0.4 \times 10^4$  axons;  $P = 0.04$ ). Similarly, for mice, the average number of axons in saline nerves was the same as for naive nerves ( $4.6 \pm 0.1 \times 10^4$  axons;  $P = 0.60$ ), whereas microbead nerves had 20% less ( $3.7 \times 10^4$  axons;  $P = 0.04$ ). Thus, sustained elevations in IOP induced by microbead injections resulted in modest but measurable thinning of the axon population in the optic nerve. For simplicity, Figure 6C shows axon density and axon number as ratios (left to right eyes) for

both rats and mice. For naive samples, the two eyes were identical for all measurements, leading to ratios close to unity ( $P \geq 0.35$ ).

## DISCUSSION

In this study, we describe a means for the induction of modest ocular hypertension in rodents in which both the magnitude and the duration of IOP elevation can be reliably manipulated by the injection of polystyrene microbeads into the anterior chamber (Fig. 1). Our model builds on a limited number of earlier studies using microbeads to elevate IOP in primates,<sup>20</sup> rats,<sup>21</sup> and rabbits.<sup>22</sup> In our paradigm, microbead injection was



limited to one eye, with the other eye receiving an equivalent volume of saline. This serves as a convenient internal control for the surgical procedure except for the microbeads themselves. Examination of the anterior segment after injection suggests that the microbeads could have been carried by the flow of aqueous humor into the region of the trabecular meshwork, where they congregated (Fig. 1). Although microbead injection elicited reliable elevations in IOP for both rats and mice, equivalent-volume injections of saline in the fellow eye had little or no lasting effect on IOP. It is reasonable to conclude that elevations in IOP observed in the microbead-injected eye are the result of impeded outflow rather than an increase in general volume of the anterior segment or some other facet of the surgical procedure (i.e., inflammation or corneal wound healing). The relatively small day-to-day variability once IOP is elevated can be explained by simple persistence of the microbeads near the outflow region. This remains to be tested explicitly.

We found that the magnitude of IOP elevation in rats, as measured by tonometry, could be controlled by varying the injection volume because larger volumes (i.e., more microbeads) induced a higher elevation. For example, in the rat, a single 2.5- $\mu$ L injection of microbeads elevated IOP on average by  $4.4 \pm 1.3$  mm Hg compared with  $7.2 \pm 0.8$  mm Hg for a 5- $\mu$ L injection ( $P < 0.001$ ). These increments represented a 21% and a 34% increase, respectively, compared with the saline companion eye (Figs. 2, 3). Increasing the volume to 7  $\mu$ L did not significantly increase IOP compared with 5  $\mu$ L (Fig. 3A). The elevation in IOP afforded by a single 5- $\mu$ L injection persisted for approximately 2 weeks, with a statistically linear accumulation of pressure exposure during this period (Figs. 3B, C). A second 5- $\mu$ L injection elevated IOP up to an additional 6 weeks, with a magnitude and a rate of accumulation of pressure exposure very similar to that of a single injection (Figs. 4C, D). Thus, two 5- $\mu$ L injections can elicit a near constant elevation in IOP for approximately 8 weeks (Fig. 4E). That the period of elevation afforded by a second 5- $\mu$ L injection lasts so much longer probably indicates a cumulative buildup of microbeads in the outflow region that reaches some critical mass. We doubt that this elevation is permanent, but its complete duration remains to be determined in future planned experiments. As well, in this study we did not track IOP from the first injection to full recovery to baseline. Thus, though modest recovery was observed by approximately 2 weeks, the precise duration remains unknown until additional studies are completed.

For mice, we found that a single 1- $\mu$ L microbead injection could elicit a  $4.6 \pm 0.6$  mm Hg elevation above IOP for the saline eye, a 30% increment comparable to that of the rat (Figs 5A, C). This elevation could persist for slightly more than 3 weeks, affording a statistically linear accumulation in exposure to increased pressure (Fig. 5D). However, there was significant variability in the durability of this single injection that depended on the experimenter: a second cohort from a relatively newer user demonstrated IOP elevation of lower magnitude and duration (Fig. 5B). This might have resulted, for example, from the inadvertent presence of air bubbles in the injection apparatus yielding a slightly smaller injection volume. In this sense, a single 1- $\mu$ L injection for the mouse eye can have an effect similar to that of back-to-back 5- $\mu$ L injections in the larger rat eye, depending on the success of the injection. Even so, similar to the 5- $\mu$ L injection in rats, the interanimal variability was modest: on a given day, IOP varied between animals by approximately 5% of the mean.

The 30% elevation in IOP arising from microbead injection in rodents more closely resembles changes in IOP associated with mild to moderate ocular hypertension in untreated human eyes, which are on average 38% above 15 mm Hg.<sup>30</sup> In con-

trast, in other heavily used models, the magnitude of IOP elevation is frequently 50% to 100% above that of the fellow eye and is entirely dependent on the success of the surgical procedure.<sup>4,5,10</sup> Combined with its reliability after microbead injection, the less severe magnitude of IOP elevation could prove useful in identifying subtle aspects of the early response in glaucoma. We found that the 30% elevation in IOP elicited a modest but measurable thinning of the axon population in the optic nerve for both rats and mice after 4 to 5 weeks (Fig. 6). This thinning was concurrent with signs of the typical hallmarks of glaucomatous pathology (gliosis, degenerating profiles, disorganization), which also were modest compared with other models. Because such incremental changes could present a problem to preclinical testing of neuroprotective interventions, more extensive studies are under way to determine whether nerve abnormalities continue to progress with a more extensive period of IOP elevation.

### Acknowledgments

The authors thank Quintus Ngumah at the University of Alabama Birmingham for early advice on technique and the Vanderbilt University Medical Center Cell Imaging Shared Resource core facility for support with confocal imagery.

### References

- Coleman AL, Miglior S. Risk factors for glaucoma onset and progression. *Surv Ophthalmol*. 2008;53(suppl 1):S3-S10.
- Kass MA, Heuer DK, Higginbotham EJ, et al. The ocular hypertension treatment study—a randomized trial determines that topical ocular hypotensive medication delays or prevents the onset of primary open angle glaucoma. *Arch Ophthalmol*. 2002;120:701-713.
- Jonas JB, Budde WM. Diagnosis and pathogenesis of glaucomatous optic neuropathy: morphological aspects. *Prog Retinal Eye Res*. 2000;19:1-40.
- Morrison JC. Elevated intraocular pressure and optic nerve injury models in the rat. *J Glaucoma*. 2005;14:315-317.
- Pang IH, Clark AF. Rodent models for glaucoma retinopathy and optic neuropathy. *J Glaucoma*. 2007;16:483-505.
- McKinnon SJ, Schlamp CL, Nickells RW. Mouse models of retinal ganglion cell death and glaucoma. *Exp Eye Res*. 2009;88:816-824.
- Morrison JC, Moore CG, Deppmeier LM, et al. A rat model of chronic pressure-induced optic nerve damage. *Exp Eye Res*. 1997;64:85-96.
- Nissirios N, Chanis R, Johnson E, et al. Comparison of anterior segment structures in two rat glaucoma models: an ultrasound biomicroscopic study. *Invest Ophthalmol Vis Sci*. 2008;49:2478-2482.
- Goldblum D, Mittag T. Prospects for relevant glaucoma models with retinal ganglion cell damage in the rodent eye. *Vision Res*. 2002;42:471-478.
- Ueda J, Sawaguchi S, Hanyu T, et al. Experimental glaucoma model in the rat induced by laser trabecular photocoagulation after an intracameral injection of India ink. *Jpn J Ophthalmol*. 1998;42:337-344.
- Levkovitch-Verbin H, Quigley HA, Martin KR, et al. Translimbal laser photocoagulation to the trabecular meshwork as a model of glaucoma in rats. *Invest Ophthalmol Vis Sci*. 2002;43:402-410.
- Aihara M, Lindsey JD, Weinreb RN. Experimental mouse ocular hypertension: establishment of the model. *Invest Ophthalmol Vis Sci*. 2003;44:4314-4320.
- Grozdanic SD, Betts DM, Sakaguchi DS, et al. Laser-induced mouse model of chronic ocular hypertension. *Invest Ophthalmol Vis Sci*. 2003;44:4337-4346.
- Sawada A, Neufeld AH. Confirmation of the rat model of chronic moderately elevated intraocular pressure. *Exp Eye Res*. 1999;69:525-531.
- Bayer AU, Danias J, Brodie S, et al. Electroretinographic abnormalities in a rat glaucoma model with chronic elevated intraocular pressure. *Exp Eye Res*. 2001;72:667-677.

16. Shareef SR, Garcia-Valenzuela E, Salierno A, et al. Chronic ocular hypertension following episcleral venous occlusion in rats. *Exp Eye Res.* 1995;61:379-382.
17. Mittag TW, Danias J, Pohorenc G, et al. Retinal damage after 3 to 4 months of elevated intraocular pressure in a rat glaucoma model. *Invest Ophthalmol Vis Sci.* 2000;41:3451-3459.
18. Yu S, Tanabe T, Yoshimura N. A rat model of glaucoma induced by episcleral vein ligation. *Exp Eye Res.* 2006;83:758-770.
19. Benozzi J, Nahum LP, Campanelli JL, et al. Effect of hyaluronic acid on intraocular pressure in rats. *Invest Ophthalmol Vis Sci.* 2002;43:2196-2200.
20. Weber AJ, Zelenak D. Experimental glaucoma in the primate induced by latex microspheres. *J Neurosci Methods.* 2001;111:39-48.
21. Urcola JH, Hernandez M, Vecino E. Three experimental glaucoma models in rats: comparison of the effects of intraocular pressure elevation on retinal ganglion cell size and death. *Exp Eye Res.* 2006;83:429-437.
22. Ngumah QC, Buchthal SD, Dacheux RF. Longitudinal non-invasive proton NMR spectroscopy measurement of vitreous lactate in a rabbit model of ocular hypertension. *Exp Eye Res.* 2006;83:390-400.
23. Jia L, Cepurna WO, Johnson EC, et al. Effect of general anesthetics on IOP in rats with experimental aqueous outflow obstruction. *Invest Ophthalmol Vis Sci.* 2000;41:3415-3419.
24. Sappington RM, Sidorova T, Long DJ, Calkins D. TRPV1: contribution to retinal ganglion cell apoptosis and increased intracellular  $Ca^{2+}$  with exposure to hydrostatic pressure. *Invest Ophthalmol Vis Sci.* 2009;50:717-728.
25. Sappington RM, Calkins DJ. Contribution of TRPV1 to microglia-derived IL-6 and NF $\kappa$ B translocation with elevated hydrostatic pressure. *Invest Ophthalmol Vis Sci.* 2008;49:3004-3017.
26. Inman DM, Sappington RM, Horner PJ, Calkins DJ. Quantitative correlation of optic nerve pathology with ocular pressure and corneal thickness in the DBA/2 mouse model of glaucoma. *Invest Ophthalmol Vis Sci.* 2006;47:986-996.
27. McKinnon SJ, Lehman DM, Kerrigan-Baumrind LA, et al. Caspase activation and amyloid precursor protein cleavage in rat ocular hypertension. *Invest Ophthalmol Vis Sci.* 2002;43:1077-1087.
28. Mermoud A, Baerveldt G, Minckler DS, Prata JA Jr, Rao NA. Aqueous humor dynamics in rats. *Graefes Arch Clin Exp Ophthalmol.* 1996;234(suppl 1):S198-S120.
29. Zhang D, Vetrivel L, Verkman AS. Aquaporin deletion in mice reduces intraocular pressure and aqueous fluid production. *J Gen Physiol.* 2002;119:561-569.
30. Sommer A, Tielsch JM, Katz J, et al. Relationship between intraocular pressure and primary open angle glaucoma among white and black Americans: the Baltimore Eye Survey. *Arch Ophthalmol.* 1991;109:1090-1095.